

GRAIN SIZE EFFECT ON THE MAGNETIC AND ELECTRICAL PROPERTIES OF THE BILAYER $\text{LaSr}_2\text{Mn}_2\text{O}_7$ MANGANITE PREPARED BY SOL-GEL METHOD

M. H. EHSANI, M. E. GHAZI^{a*}, P. KAMELI^b

Department of physics, Shahrood University of Technology, Shahrood, 36155-316, Iran

^aDepartment of physics, Shahrood University of Technology, Shahrood, 36155-316, Iran

^bDepartment of physics, Isfahan University of Technology, Isfahan 84156-8311, Iran

The bilayer manganite $\text{LaSr}_2\text{Mn}_2\text{O}_7$ with different grain sizes (nano to micro scale) are prepared by sol-gel method. The effect of grain size on the magnetic and electrical properties of samples is studied using ac susceptibility and resistivity measurements. The ac susceptibility measurement results show the effect of grain size on magnetic ordering phases. By increasing the grain size, high temperature long-range charge ordering phase along with low temperature anti-ferromagnetic spin couple phase appear in the sample. Also resistivity measurements reveal insulating behavior for all samples in our experimental limit, and by increasing the grain size, resistivity decreases first and then increases due to the grain size effect and appearance of different magnetic phases.

(Received February 6, 2012; Accepted May 12, 2012)

Keywords: Bilayer manganites, grain size, magnetic ordering, charge exchange (CE), ac susceptibility

1. Introduction

The Ruddlesdon-Popper (RP) series manganite compounds are demonstrated with the general formula $\text{A}_{n-nx}\text{B}_{1+nx}\text{Mn}_n\text{O}_{3n+1}$, where A and B are rare-earth ions and divalent cations, respectively. In these compounds, n is the number of MnO_6 octahedral layers in the unit cell that is alternately stacked with $(\text{A,B})_2\text{O}_2$ layers along the C axis of the structure, whereas in the case of cubic $\text{La}_{1-x}\text{A}_x\text{MnO}_3$, the MnO_6 octahedral extends all over the space.

The $n=1$ member, $\text{A}_{1-x}\text{B}_{1+x}\text{MnO}_4$, has two-dimensional (2D) K_2NiF_4 -type structure and the $n=2$ member, $\text{A}_{2-2x}\text{B}_{1+2x}\text{Mn}_2\text{O}_7$, has the quasi-2D $\text{Sr}_3\text{Ti}_2\text{O}_7$ -type tetragonal structure, which is known as bilayer manganite. The $n=\infty$ member, $\text{A}_{1-x}\text{B}_x\text{MnO}_3$ (3D manganite), is generally described by perovskite structure [1-10].

Manganites are considerably studied because of their unique properties such as Jahn-Teller effect, colossal magnetoresistance (CMR), metal-insulator transition, and so on [11-16]. The 3D manganites were discovered 60 years ago by Jonker et al. [17], and since then, many papers have been published about their properties. Bilayer manganites were discovered by Moritomo et al. in 1996 [2]. In comparison with 3D manganites, bilayer manganites demonstrate anisotropy in their structure. Due to this structural anisotropy, it should present anisotropy in physical properties, including magnetic and transport ones [18-21].

Real space charge ordering (CO) and appearance of anti-ferromagnetic (AFM) spin ordering below the CO transition temperature, T_{CO} , are the most interesting phenomena in

* Corresponding author: ebrahim_ghazi@yahoo.com

manganites [22]. The 50% doped bilayer manganite, $\text{LaSr}_2\text{Mn}_2\text{O}_7$, shows AFM spin ordering and CO below 210 K and 140 K, respectively [23, 24]. The CO state can be controlled by chemical and physical methods. For example, substitution of the non-magnetic ion Ti for Mn in $\text{LaSr}_2\text{Mn}_2\text{O}_7$ suppresses the CO and AFM transition temperature [24].

In the case of 3D manganites, the results show that grain size has considerable effects on the structural, magnetic, and electrical properties of samples [25-28]. For example, Zhang et al. observed reduction of CO transition temperature by decreasing grain size of the $\text{La}_{0.25}\text{Ca}_{0.75}\text{MnO}_3$ sample, indicating weakening of the CO state [25]. To the best of our knowledge, few reports have been published on effects of the grain size of bilayer compounds on physical properties until now. Tasarkuyu *et al.* have reported increase in the Curie temperature and magnetic entropy of $\text{La}_{1.4}\text{Ca}_{1.6}\text{Mn}_2\text{O}_7$ bilayer by increasing the grain size [29]. In this work, we investigated the grain size effect on the structural, magnetic, and transport behaviors of $\text{LaSr}_2\text{Mn}_2\text{O}_7$ polycrystalline samples.

2. Experimental

$\text{LaSr}_2\text{Mn}_2\text{O}_7$ fine powders were prepared by Pichini sol-gel method. All chemicals (analytical grade reagents) were purchased from Merck Company, and used as received without further purification. Highly pure powders of the nitrate precursor reagents $\text{La}(\text{NO}_3)_3 \cdot 6\text{H}_2\text{O}$, $\text{Mn}(\text{NO}_3)_2 \cdot 4\text{H}_2\text{O}$ and $\text{Sr}(\text{NO}_3)_2$, weighted in appropriate proportions, were used to obtain $\text{LaSr}_2\text{Mn}_2\text{O}_7$. All the nitrates were dissolved in distilled water under continuous stirring. Then aqueous solution of citric acid as a complexation agent (4 mol for 1 mol of metal ions) and ethylene glycol as a polymerization agent (3 mol for 1 mol on metal ions) were added to the main solution. The solution was stirred and the pH of solution adjusted to 5-6 by adding ammonia solution. On slow stirring of the solution at 120 °C on a hot plate; a homogenous yellowish gel was obtained. The gel was dried at 180 °C in air for 18 h to obtain xerogel. To remove the organic elements, the gel was further heated and dried at 200 °C, resulting in porous foam, which was decomposed at 450 °C in an electrical oven. The powders were produced through calcining the precursors in a Carbolite tube furnace at 1200 °C for 10 h. The black powder obtained was cold pressed into pellets with diameter of 10 mm and thickness of about 2-3 mm under a pressure of 20 Tone/cm^2 . In order to study the effect of grain size on structural, magnetic, and electrical properties of the samples, the pellets were sintered for 6 h at different temperatures, $T_s = 1250$ °C (sample S-1250), 1350 °C (sample S-1350), and 1450 °C (sample S-1450).

Resistivity measurements were carried out by the four probe method, using a Leybold Closed Cycle Refrigerator. The ac susceptibility measurements were performed using a Lake Shore Ac Susceptometer Model 7000. X-ray diffraction (XRD) patterns of samples were taken on ADVANCE D-8 X-ray Diffractometer. The microstructures of samples were analyzed by a field emission scanning electron microscope (FE-SEM).

3. Results and discussion

3.1. Structural properties

Figure 1 shows XRD patterns of the samples at room temperature. The XRD data was analyzed with Rietveld refinement using the FULLPROF software and Pseudo-Voigt function. Inset of Figure 1 shows the Rietveld analysis of sample S-1450. It was found that all the diffraction peaks could be indexed using $\text{Sr}_3\text{Ti}_2\text{O}_7$ -type tetragonal structure with $I4/mmm$ space group. It is to be noted that there are some minor picks in the XRD pattern of sample S-1250, which are related to the La_2O_3 impurity phase. It can be seen that by increasing the sintering temperature, the impurity phase disappears and the intensity of XRD peaks increases, indicating the enhancement of crystallite size. The results of the Rietveld refinement were tabulated in Table 1.

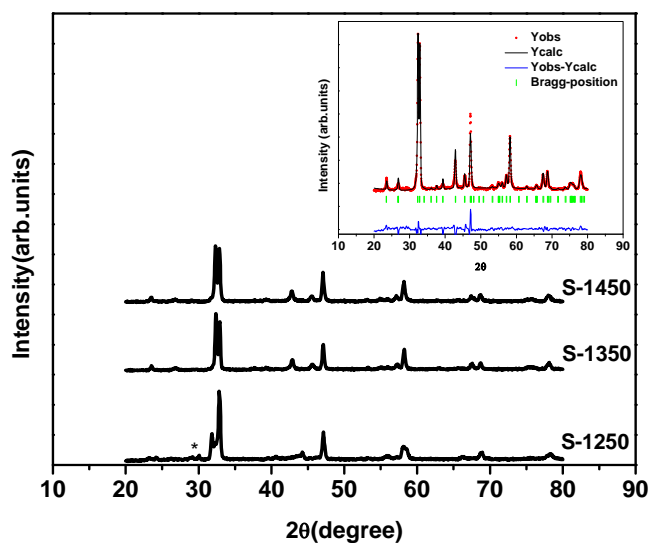


Fig. 1: XRD patterns for samples S-1250, S-1350, and S-1450. The inset shows the Rietveld refinement for sample S-1450.

The data for S-1350 and S-1450 are in good agreement with the earlier works [28, 30-32]. It is evident that the unit cell volume of sample S-1250 turns out to be compressed when compared to samples S-1350 and S-1450. This kind of behavior is in agreement with earlier works on perovskite manganites [27-33]. In fact, by decreasing the crystallite size, the lattice parameters and the unit cell volume decrease due to the surface and finite size effects.

Table 1: Lattice parameters of samples.

	a (Å)	c (Å)	V (Å ³)
S-1250	3.820	20.270	295.788
S-1350	3.860	19.940	297.098
S-1450	3.860	19.940	297.098

The FE-SEM images of the powdered samples are shown in Fig. 2. Sample S-1250 shows smaller particles with an average size of ~150 nm. By increasing the sintering temperature from 1250 °C to 1350 °C and 1450 °C, the average particle size increases from ~150 nm to ~400 nm and ~1000 nm, respectively.

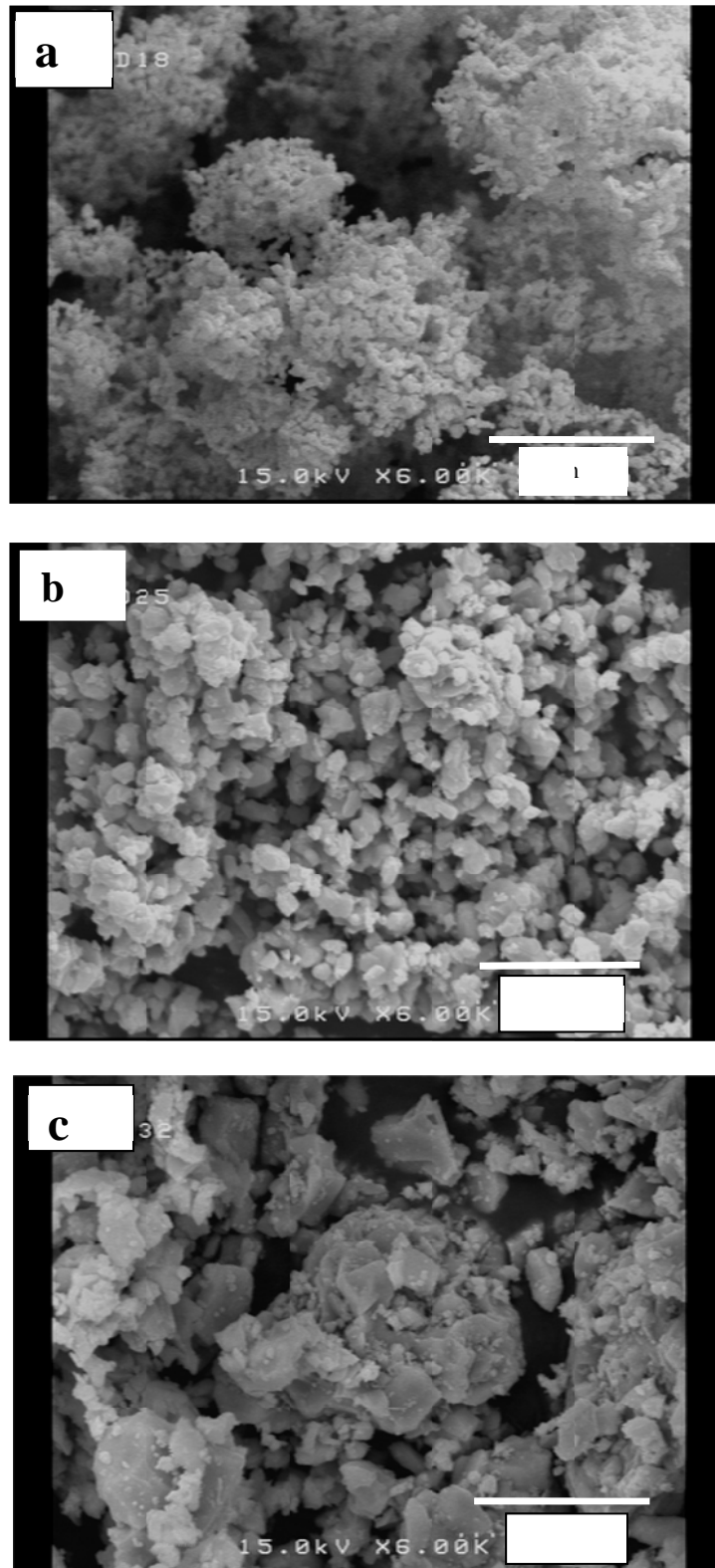


Fig. 2: FE-SEM images of the powdered samples (a) S-1250, (b) S-1350, and (c) S-1450.

3.2. Magnetic and electrical properties

The temperature dependence of ac susceptibility (real and imaginary parts) was measured for all samples in an ac field of 400 A/m and frequency of 333 Hz. Fig. 3 shows the results of the ac susceptibility measurements for sample S-1250. It is evident that upon cooling from room temperature, both parts of ac susceptibility for sample S-1250 display relatively broad maximum

at about 230 K, corresponding to the CE-type CO transition temperature, T_{CO} . It seems that in this small particle sized sample, the long-range CO phase is absent.

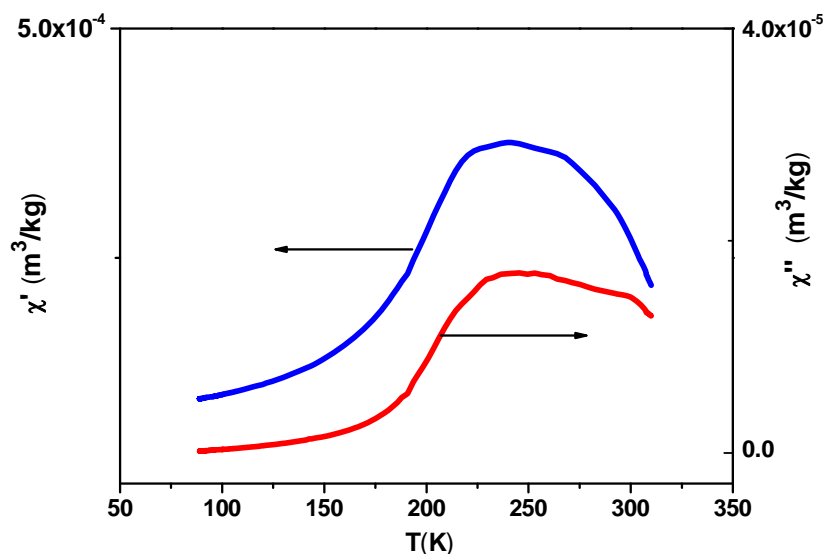


Fig. 3: Temperature dependence of ac susceptibility for sample S-1250: real part (left axis), and imaginary part (right axis).

The results of the ac susceptibility measurements for sample S-1350 is shown in Fig. 4. By increasing the sintering temperature from 1250 °C to 1350 °C, one can see different behavior of the ac susceptibility of sample S-1350. There are two differences in ac susceptibility of this sample compared to S-1250. First, the CO transition peak in sample S-1350 becomes relatively narrow, and there is oscillating magnetic behavior around T_{CO} . This oscillating behavior might be caused by rotation of Mn spins due to charge-lattice (C-L) fluctuations, which are dynamic around the CO state. This oscillating behavior was observed in other charge ordered bilayers and 3D manganites [34-38]. Secondly, by further decreasing temperature, a new peak was created around ~115 K in the imaginary part of ac susceptibility. It seems that this peak is related to AFM spin couple transition [23, 24].

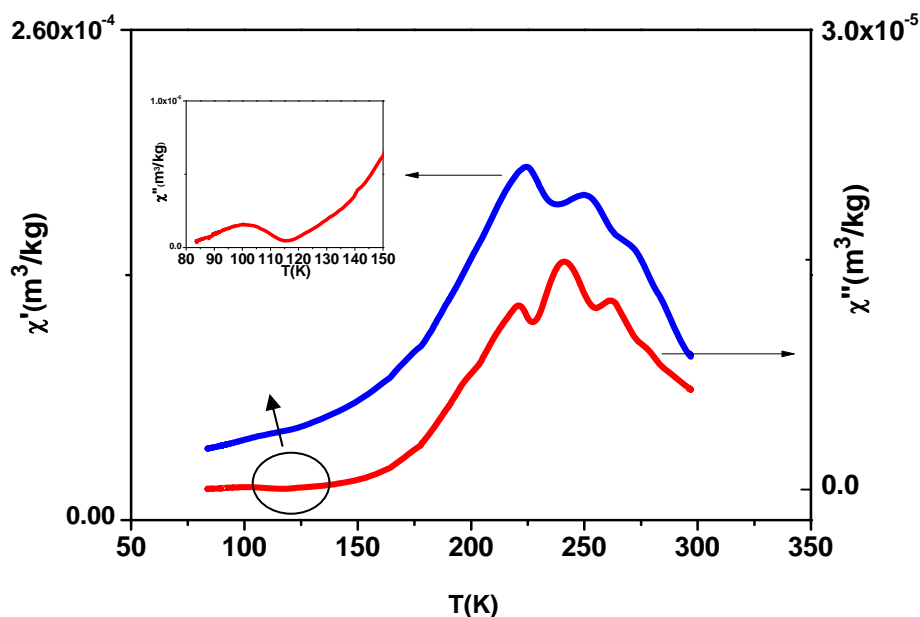


Fig. 4: Temperature dependence of ac susceptibility for sample S-1350: real part (left axis), and imaginary part (right axis).

Fig. 5 shows ac susceptibility (both real and imaginary parts) as a function of temperature for sample S-1450. As it can be seen in this figure, the oscillating behavior is absent in this sample. Also the CO transition width becomes sharp, and AFM spin couple transition is clearly seen in both parts of the ac susceptibility. The results of the ac susceptibility measurements indicate that by increasing the particle size (sintering temperature), the CE-type CO phase becomes long range and stable. At the same time, the volume fraction of the low temperature AFM spin couple phase increases considerably. The effect of particle size was observed in several charge ordered 3D manganites such as $\text{La}_{0.5}\text{Ca}_{0.5}\text{MnO}_3$ [27], $\text{Bi}_{0.2}\text{Ca}_{0.8}\text{MnO}_3$ [28], and $\text{Pr}_{0.5}\text{Ca}_{0.5}\text{MnO}_3$ [26]. The published results show that with decreasing particle size, the CO transition becomes increasingly wide and weak.

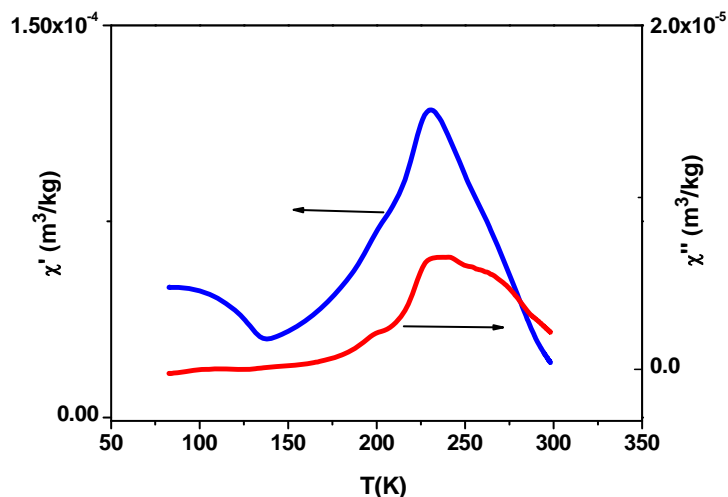


Fig.5: Temperature dependence of ac susceptibility for sample S-1450: real part (left axis), and imaginary part (right axis).

Temperature dependence of resistivity for samples S-1250, S-1350, and S-1450 is given in Fig. 6. All samples exhibit insulating behavior in our experimental limit. Also by increasing the sintering temperature, resistivity of samples in all temperature ranges decrease from sample S-1250 to S-1350, and then increases for sample S-1450.

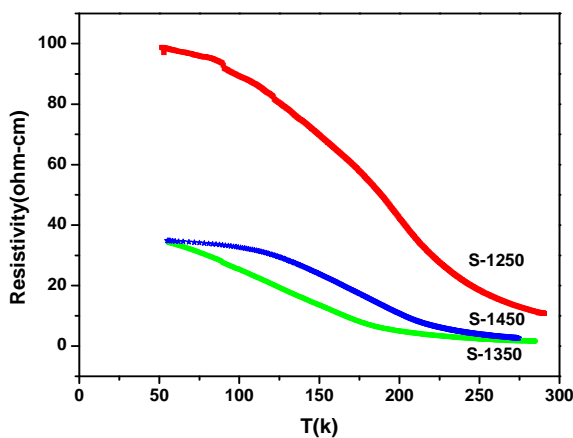


Fig. 6: Temperature dependence of resistivity for samples S-1250, S-1350, and S-1450.

This could be explained by considering grain size effect and magnetic phases. As discussed in literatures [39-41], there are two kinds of conduction channels, connected in parallel in polycrystalline manganites. One is related to intragrain, and the second one is related to intergrain, hopping the conduction electron between the neighboring sites. Furthermore, resistance of grain boundaries is more than that inside the grains because of the disorder nature of the grain boundaries. Thus as the grain size increases by increasing the sintering temperature, resistivity decreases significantly in samples S-1350 and S-1450. However, resistivity of sample S-1450 is higher than that for sample S-1350 at high temperatures, and converges to S-1350 value at low temperatures. This may be explained by considering the magnetic behaviors of the samples. Due to the long-range CO insulating phase at high temperatures (around 230 K) in sample S-1450, resistivity of this sample is higher than that for sample S-1350. However, at low temperatures, due to the appearance of AFM spin couple ordering, resistivity of this sample becomes relatively smooth. In vicinity of 140 K, in sample S-1450, we could observe a clear trend in decline in resistivity, indicating the coexistence of the CE-type CO and AFM spin couple ordering.

4. Conclusion

LaSr₂Mn₂O₇ bilayer manganite samples with different grain sizes were prepared by sol-gel method. The XRD and FESEM analyses showed that the grain size increased by increasing the sintering temperature. The ac susceptibility measurements showed that the grain size of samples affected the magnetic ordering phases. By increasing the grain size from nano-scale to micro-scale, the high temperature long range charge ordering along with the low temperature anti-ferromagnetic spin couple phase appeared in the sample. Also the resistivity measurements results showed that all samples displayed insulating behavior by decreasing temperature, and by increasing the grain size, the resistivity decreased firstly and then increased due to the grain size effect and appearance of different magnetic phases.

References

- [1] S. N. Ruddlesden and P. Popper, *Acta Crystallogr.* **11**, 54 (1958).
- [2] Y. Moritomo, A. Asamitsu, H. Kuwahara, Y. Tokura, *Nature (London)*. **383**, 41 (1996).
- [3] R. Mahash, R. Mahendiran, A. K. Raychaudhuri, and C. N. R. Rao, *J. Solid State Chem.* **122**, 448 (1996).
- [4] H. Asano, J. Hayakawa, and M. Matsui, *Phys. Rev. B* **57**, 1052 (1998).
- [5] B. J. Sternlieb, J. P. Hill, U. C. Wildgruber, G. M. Luke, B. Nachumi, Y. Moritomo, and Y. Tokura, *Phys. Rev. Lett.* **76**, 2169 (1996).
- [6] D. N. Argyriou, J. F. Mitchell, C. D. Potter, S. D. Badr, R. Kleb, and J. D. Jorgensen, *Phys. Rev. B* **55**, R11 965(1997).
- [7] R. Seshadri, A. Maignan, M. Hervieu, N. Nguyen, and B. Raveau, *Solid State Commun.* **101**, 453(1997).
- [8] K. B. Garge, N. L. Saini, B. R. Sekhar, R. K. Singhal, B. Doyle, S. Nannarone, F. Bondino, E. Magnano, E. Carleschi, and T. Chatterji, *J. Phys.:condens. Matter.* **20**, 055215 (2008).
- [9] R. Kajimoto, H. Yoshizawa, H. Kawano, H. Kuwahara, Y. Tokura, K. Ohoyama, M. Ohashi, *Phys. Rev. B* **60**, 9506(1999).
- [10] P. Schiffer, A. P. Ramirez, W. Bao, and S- W. Cheong, *Phys. Rev. Lett.* **75**, 33369 (1995).
- [11] C. Zener, *Phys. Rev.* **82**, 403(1951).
- [12] P. W. Anderson, and H. Hasegawa, *Phys. Rev.* **100**, 675 (1955).
- [13] A. J. Millis, P. B. Littlewood, and B. I. Shraimam, *Phys. Rev. Lett.* **74**, 5144 (1995).
- [14] Y. Shimakawa, Y. Kubo, and T. Manako, *Nature (London)* **379**, 53 (1996).
- [15] S. W. Cheong, H. Y. Hwang, B. Batlogg, and L. W. Rupp, *J. Solid State Commun.* **98**, 163(1966).
- [16] E. Dagotto, *New J. Phys.* **7**, 67(2005).
- [17] G. Jonker, and J. Van Santen, *Physica* .**16**, 337 (1950).
- [18] T. G. Perring, G. Aeppli, Y. Moritomo, and Y. Tokura, *Phys. Rev. Lett.* **78**, 3197(1997).
- [19] T. J. Zhou, Z. Yu, S. Y. Ding, L. Qiu, Y. W. Du, *Appl. Phys. A* **74**, 163(2002).

- [20] H. Zhu, D. Zhu, Y. Zhang, *J. Appl. Phys.* **92**, 7353(2002).
- [21] K. Hirota, Y. Moritomo, H. Fujioka, M. Kubota, H. Yoshizawa, Y. Endoh, *J. Phys. Soc. Jpn.* **67**, 3380(1998).
- [22] J. B. Goodenough, *Phys. Rev.* **100**, 555(1955).
- [23] J. F. Mitchell, D. N. Argyriou, A. Berger, K. E. Gray, R. Osborn, U. Welp, *J. Phys. Chem. B* **105**, 10731(2001).
- [24] J. Feng, P. Che, J. P. Wang, M. F. Lu, J. F. Liu, X. Q. Cao, J. Meng, *J. Alloys & Comp.* **397**, 220(2005).
- [25] T. Zhang, T. F. Zhou, T. Qian, and X. G. Li, *Phys. Rev. B* **76**, 174415(2007).
- [26] Z. Jirak, E. Hadova, O. Kaman, K. Knizek, M. Marysko, and E. Pollert, *Phys. Rev. B* **81**, 024403(2010).
- [27] T. Sarkar, B. Ghosh, and A. K. Raychaudhuri, T. Chatterji, *Phys. Rev. B* **77**, 235112 (2008).
- [28] J. Fang, Q. Wang, Y. Zou, X. Yu, R. Li, and Y. Zhang, *J. Appl. Phys.* **104**, 123905(2008).
- [29] E. Tasarkuyu, A. Coskun, A. E. Irmak, S. Akturk, G. Unlu, Y. Samancioglu, A. Yucel, C. Sarikurkcü, S. Aksoy, M. Acet, *J. Alloys & Comp.* doi:10.1061/j.jallcom.2010.12.011.
- [30] S. Nair, and A. Banerjee, *Phys. Rev. B* **70**, 1044289(2004).
- [31] R. L. Zhang, B. C. Zhao, W. H. Song, Y. Q. Ma, J. Yang, Z. G. Sheng, J. M. Dai, and Y. P. Sun, *J. Appl. Phys.* **96**, 4965(2004).
- [32] A. A. Yaremchenko, D. O. Bannikov, A. V. Kovalevsky, V. A. Cherepanov, V. V. Kharton, *J. Solid State Chem.* **181**, 3024(2008).
- [33] T. Zhang, M. Dressel, *Phys. Rev. B* **80**, 014435 (2009).
- [34] A. K. Gupta, R. Kumar, V. Kumar, G. L. Bhalla, N. Khare, *J. Physics and Chemistry of Solids.* **70**, 117(2009).
- [35] M. Matsukawa, E. Kikuchi, M. Yoshizawa, M. Apostu, R. Suryanarayanan, A. Revcolevschi, N. Kobayashi, *Physica B* **329-333**, 900 (2003).
- [36] N. Mohapatra, S. N. Bhatia, D. C. Kundaliya, S. K. Malik, *Physica B* **359-361**, 1285(2005).
- [37] S. Y. Wu, W. H. Li, K. C. Lee, H. D. Yang, *Physica B* **259-261**, 839(1999).
- [38] R. Kajimoto, T. Kakeshita, Y. Ohara, and H. Yoshizawa, Y. Tomioka, Y. Tokura, *Phys. Rev. B.* **58**, R11 837(1998).
- [39] M. M. Rubinsten, *J. Appl. Phys.* **87**, 5019 (2000).
- [40] D. Das, C. M. Srivastava, D. Bahadur, A. K. Nigam, S. K. Malik, *J. Phys. Condens Matter.* **16**, 4089 (2004).
- [41] M. Eshraghi, H. Salamati, P. Kameli, *J. phys.: Condens. Matter.* **18**, 8281 (2006).